Low-energy fusion hindrance in medium-light systems

Giovanna Montagnoli[1,2,*]

[1]Department of Physics and Astronomy, University of Padua
[2]INFN - Section of Padua

Abstract. Heavy-ion fusion reactions give fundamental information on the quantum tunnelling of many-body systems where several intrinsic degrees of freedom are contributing. Moreover, the existence of hindrance in the fusion of light systems is critical for a variety of stellar environments.
Hindrance is often characterised by a maximum of the astrophysical S factor with decreasing energy, and is an interesting link between heavy-ion fusion and astrophysics. The underlying physical background is still under debate. Recently it has been pointed out that the Pauli exclusion principle influences the ion-ion potential and, as a consequence, low-energy fusion hindrance is produced because of the thicker and higher Coulomb barrier. We recently performed systematic investigations on the fusion of several medium-light systems to establish a reliable basis for the extrapolation to the lighter cases of astrophysical interest. The results obtained for ^{12}C + ^{24,26}Mg and ^{12}C + ^{30}Si are discussed here. Hindrance is observed in all cases, however, with differing features, so extrapolating to lighter systems is not straightforward. Additionally, oscillations are observed in the sub-barrier logarithmic slopes of the ^{12}C + ^{24,26}Mg excitation functions, which complicates identifying the hindrance threshold in those two cases.
Coupled-channels calculations for all these systems have been performed. The results show that fusion cross sections are well reproduced by simple tunnelling through the potential barrier, at the lowest energies. An alternative way to represent the data is discussed, which helps identifying the various channel couplings.

1 Introduction

The fusion hindrance phenomenon far below the barrier was first observed about 20 years [1] ago for the system ^{60}Ni + ^{89}Y. Fusion hindrance is recognized in many cases by the trend of the logarithmic slope of the excitation function or by a maximum of the S-factor at low energies. Alternatively, a comparison with standard Coupled-Channels (CC) calculations can help to identify the phenomenon which has been observed even in light systems, e.g. in ^{12}C + ^{24,26}Mg,^{30}Si.

The case of ^{64}Ni + ^{64}Ni [2] was studied down to ≃20 nb, and its behaviour is shown in Fig. 1 (top). We see that standard CC calculations based on a Woods-Saxon potential overpredict the low-energy cross sections. Moreover, the astrophysical S-factor develops a maximum at the energy where the logarithmic slope L(E) reaches the value $L_{CS} = \pi\eta/E$. This energy has often been phenomenologically taken as the threshold for the hindrance effect. The bottom panel of the same figure shows that when moving to lighter systems L(E) and L_{CS} are two nearly parallel curves so the crossing point (if existing) is rather undetermined. As a consequence the S-factor maximum becomes broader and the hindrance threshold is difficult to be recognized.

Please note that for such light systems having positive fusion Q-value the existence of an S-factor maximum is not algebraically necessary. Indeed, the existence of fusion hindrance in those cases is neither well-established nor understood. Relevant examples are shown in Fig. 2. In the case of ^{12}C + ^{12}C, it is not easy to recognise a general trend of the S-factor, not only because the data sets are not always in agreement with each other, but mainly due to the presence of many resonances. They completely disappear in ^{12}C + ^{13}C (centre) where, furthermore, the trend is not compatible with the hindrance expectation [2]. On the other hand, in the case of ^{16}O +^{16}O the experimental data might indicate the presence of a possible S-factor maximum.

2 The systems ^{12}C + ^{24,26}Mg,^{30}Si

Several medium-light systems have been the object of recent investigations at LNL. They have as a common feature a positive Q_{fus} and some relevant results are reported in Fig. 3. Concerning ^{12}C + ^{24}Mg we point out that fusion hindrance shows up already at 0.75mb which is a remarkably high value when placed in the systematics (see the following Fig. 6). Moreover, the lowest energy points are well reproduced by tunnelling through a one-dimensional barrier, see top panel of Fig. 3.

The hindrance threshold for ^{12}C + ^{26}Mg is significantly lower than for ^{12}C + ^{24}Mg. Actually, the two excitation functions essentially coincide above the barrier, however, the cross sections of ^{12}C + ^{26}Mg start to be larger

*e-mail: giovanna.montagnoli@unipd.it

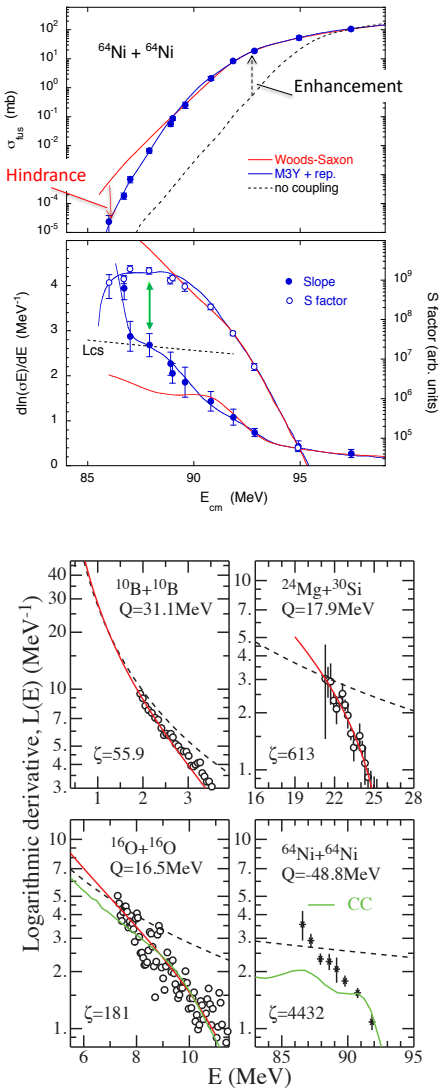

Figure 1. (top) The classical case of ^{64}Ni + ^{64}Ni where fusion hindrance clearly shows up [2]. (bottom) Logarithmic derivative vs energy for light and medium-heavy systems [3].

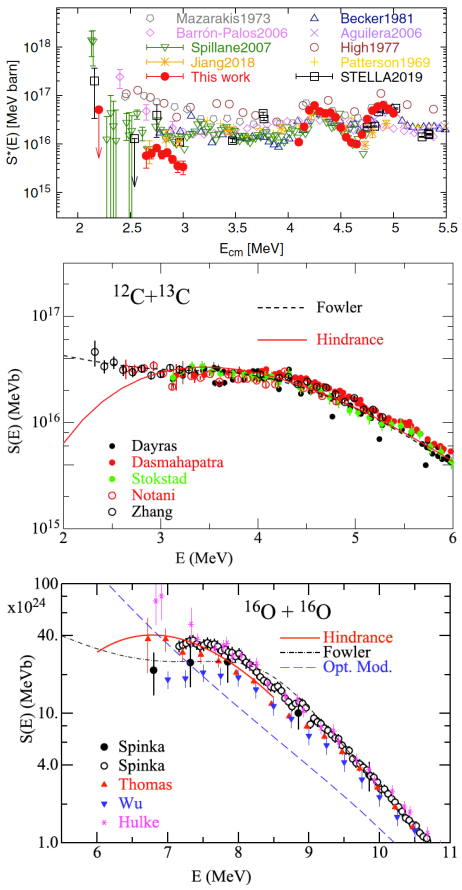

Figure 2. Astrophysical S-factors for the light systems ^{12}C + ^{12}C (top) [5], ^{12}C + ^{13}C (centre) [6] and ^{16}O +^{16}O (bottom) [4].

than for ^{12}C + ^{24}Mg from the barrier down, until they are a factor 4–5 larger at the lowest energies. This enhancement can hardly be ascribed to nuclear structure differences. Anyway, a maximum vs energy of the S-factor is observed for both systems (centre panel of Fig. 3).

The logarithmic derivatives of the two excitation functions are shown in the right panel and are very similar to each other. They are characterized by oscillations in the sub-barrier energy region. They are clearly recognisable even if the experimental uncertainties are rather large for ^{12}C + ^{24}Mg. The observed peaks appear at essentially the same energies for the two systems (see Ref. [7] for details).

Oscillations that might have an analogous origin have been observed in various lighter systems like ^{12}C + ^{12}C (see Fig. 2) or ^{12}C + ^{16}O. Several interpretations were proposed, including exotic nuclear structures like molecular states, and, more recently, it was suggested [4] that the level density in the compound nucleus might play a decisive role.

Fig. 4 shows on the top panel the level density ρ vs compound nucleus (CN) excitation energy E_x for ^{24,26}Mg + ^{12}C and ^{13}C + ^{24}Mg according to Refs. [8, 9]. The dots represent the CN excitation energies at the corresponding Coulomb barriers. One sees that the level density for ^{26}Mg + ^{12}C is larger than for ^{24}Mg + ^{12}C. This is in agreement with the previous observation that the oscillations are somewhat more damped in the first system. The level density for ^{13}C + ^{24}Mg is predicted to be much larger, so it would be quite interesting to obtain experimental data also for this case. In the same figure (bottom panel) an analogous plot is shown for ^{12}C + ^{12,13}C and ^{12}C + ^{20}Ne where the dots are the experimental values as reported in [10]. One sees that the level density of the CN for ^{12}C + ^{12}C is much lower than for ^{12}C + ^{13}C. This parallels the observation (see Fig. 2) that oscillations are only observed in the first system.

The fusion of ^{12}C + ^{30}Si is not a relevant process for astrophysics, but it is important to establish its behaviour below the barrier [11]. This system was studied a few years ago and the results are shown in Fig. 5. The excitation function is reported in the top panel, where it is compared with CC calculations performed with the CCFULL code [14]. The inset shows the lower energy points which are slightly overestimated by the CC results. The logarithmic slope and the S factor (bottom panel) have been

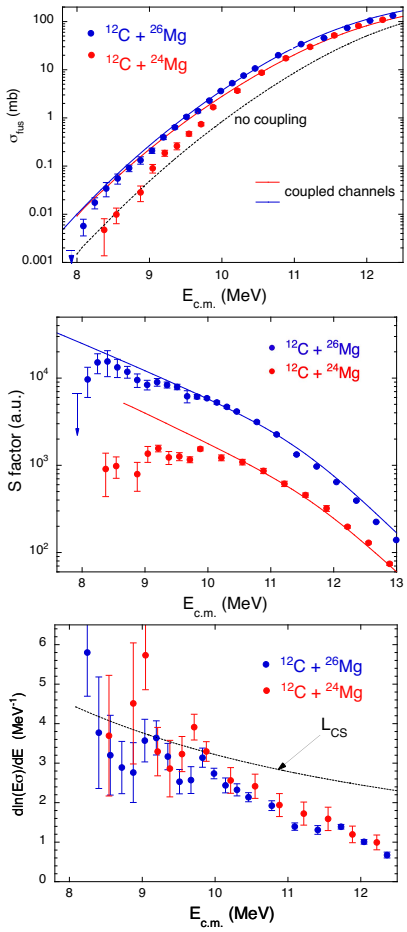

Figure 3. Fusion excitation functions (top), S-factors (centre) and logarithmic derivatives of ^{24,26}Mg + ^{12}C (bottom) [7].

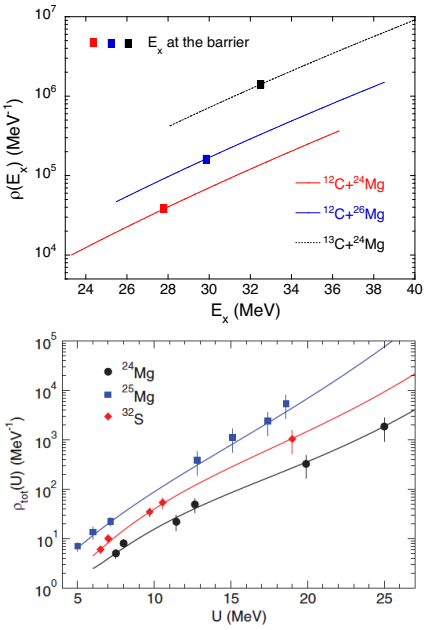

Figure 4. Level densities vs compound nucleus excitation energy for ^{24,26}Mg + ^{12}C and ^{13}C + ^{24}Mg (top) and for ^{12}C + ^{12,13}C, ^{12}C + ^{20}Ne (bottom) as predicted in Refs. [8, 9]. The dots on the right panel are experimental data.

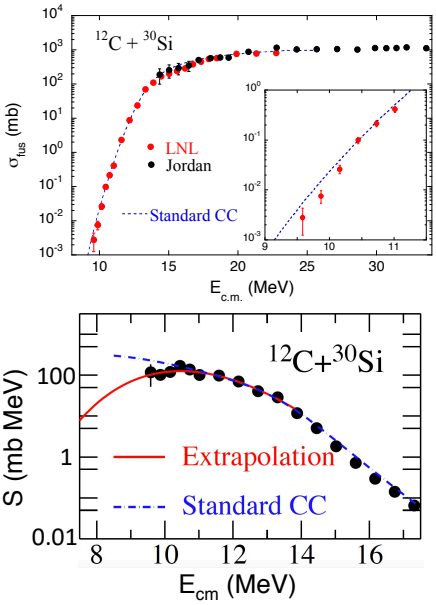

Figure 5. (top) The excitation function compared to standard CC calculations and (bottom) the trend of the astrophysical S-factor for ^{12}C + ^{30}Si [11, 12].

extracted and we have convincing phenomenological evidence of the hindrance effect.

We see from the systematics of Fig. 6 (top panel) that the system ^{12}C + ^{30}Si with Q_{fus} = +14.1 MeV has a ζ parameter very close to the lighter cases important for stellar evolution. ^{12}C + ^{24}Mg (Q_{fus} = +16.3 MeV) is even closer to them. There is a relevant difference between its hindrance threshold and the one observed for ^{12}C + ^{26}Mg (Q_{fus} = +18.5 MeV). The evidence from these three systems makes the extrapolation to the lighter cases rather uncertain.

Going to the bottom panel, we point out that the cross section at the hindrance threshold in ^{12}C + ^{24}Mg is very high ($\sigma_s \simeq 0.75$ mb), the largest observed so far among the cases where an S-factor maximum shows up clearly. In the nearby system ^{12}C + ^{30}Si the corresponding threshold cross section is about a factor 10 smaller. The same is true for ^{12}C + ^{26}Mg whose threshold is even lower. The underlying reason why this is so is still unclear.

3 Systematic trends

The ratio of measured fusion cross sections σ_{exp} to the calculated ones in the no-coupling limit is plotted in Fig. 7 vs the energy distance from the barrier for the systems ^{12}C+^{24}Mg, ^{12}C+^{30}Si, ^{48}Ca+^{48}Ca and ^{58}Ni+^{54}Fe. In all these cases the hindrance effect has been observed.

We notice that the sub-barrier enhancement is larger for the two heavier systems. While it is seen that for the two lighter cases the ratio decreases to one at the lowest energies, this does not show up for the two heavier ones. At least for ^{12}C + ^{24}Mg, ^{12}C + ^{30}Si, and at deep sub-barrier energies, fusion cross sections are well approximated by tunnelling through a one-dimensional barrier.

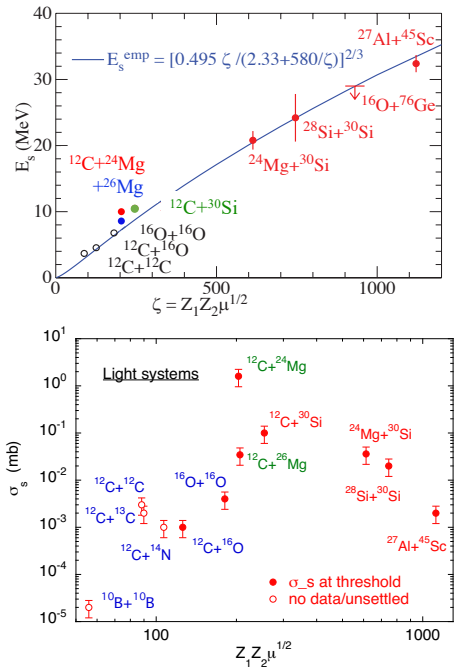

Figure 6. Threshold energies for hindrance (top) and fusion cross section at hindrance threshold (bottom) vs the parameter ζ=$Z_1Z_2\mu^{1/2}$ for medium-light systems [13]. The open dots for the lightest cases are obtained by extrapolations from higher energies.

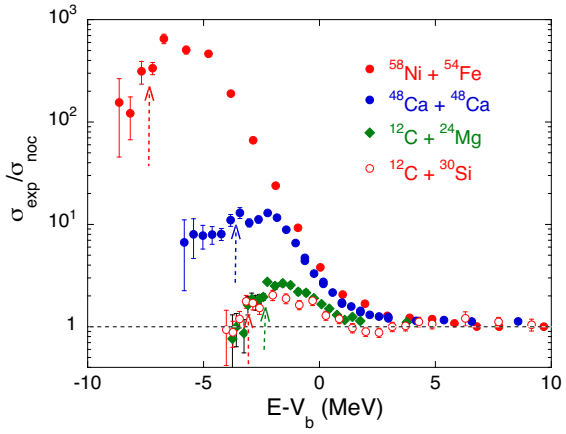

Figure 7. The ratio of the experimental cross sections to no-coupling calculations is plotted vs the energy distance from the barrier, for four systems [11, 15–17]. The vertical arrows indicate the corresponding hindrance threshold (figure reported from Ref. [17]).

Qualitatively, we can deduce that, at very low energies, the coupling strengths tend to vanish. This behaviour is predicted by the adiabatic model inside the touching point and it produces hindrance in that region where the concept of a two-body potential loses its meaning [18, 19].

4 An alternative data representation

Fig. 8 shows the fusion excitation function of three medium-heavy systems where the hindrance effect was recognized several years ago [2, 15, 20]. As a reference, the figure also reports the result of the "no coupling" calculation (dashed line), that is, the excitation function obtained by pure tunnelling through a one-dimensional barrier.

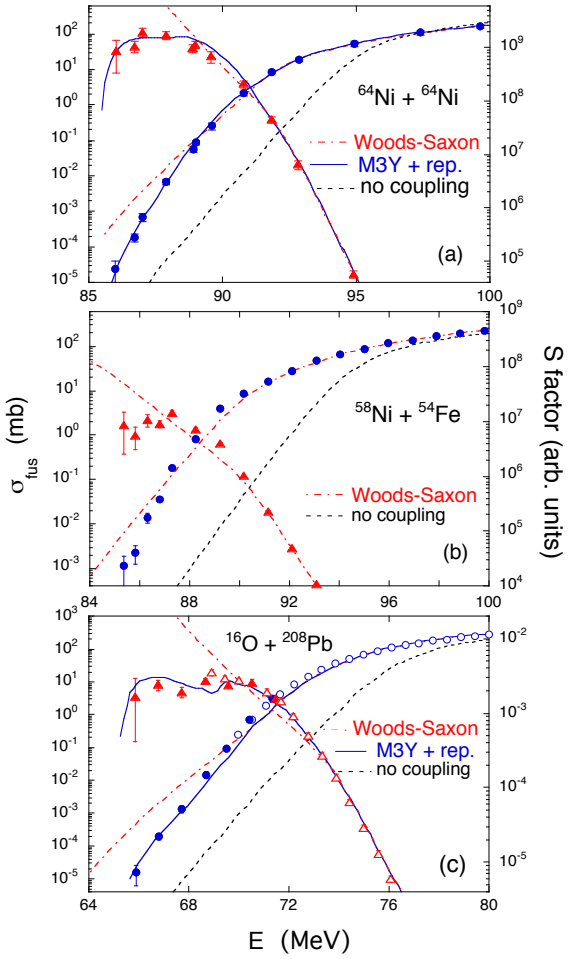

Figure 8. Fusion excitation functions and astrophysical S factors of ^{64}Ni + ^{64}Ni [2] (a), ^{58}Ni+^{54}Fe [15] (b) and ^{16}O + ^{208}Pb (c) [20], compared to CC calculations.

Using the parabolic approximation of the barrier, one obtains the Wong formula [21] which is well approximated, below the barrier, by the expression

$$E\sigma_{fus}(E) = \frac{\hbar\omega R_b^2}{2} exp\left[\frac{2\pi}{\hbar\omega}(E - V_b)\right] \qquad (1)$$

where R_b is the barrier radius and ω is the frequency related to the parabolic barrier. The energy derivative of that expression at sub-barrier energies is given by

$$\frac{d(E\sigma_{fus})}{dE} = \frac{\hbar\omega R_b^2}{2} exp\left[\frac{2\pi}{\hbar\omega}(E - V_b)\right] \frac{2\pi}{\hbar\omega} = \frac{2\pi}{\hbar\omega} E\sigma_{fus} \qquad (2)$$

Therefore, in the Wong approximation, the sub-barrier excitation function and its slope are proportional to each other, related by the quantity $2\pi/\hbar\omega$. This suggests to plot, for the same systems, the first derivative $d(E\sigma)/dE$ vs $E\sigma$ (see Fig. 9). This representation removes the effect of the varying Coulomb barrier when comparing different cases. The figure shows that the behaviour of the three systems (top panel) ^{16}O + ^{208}Pb, ^{58}Ni + ^{54}Fe and ^{64}Ni+^{64}Ni is very similar, even if they strongly differ in the mass asymmetry and for their nuclear structure. The slopes saturate at high

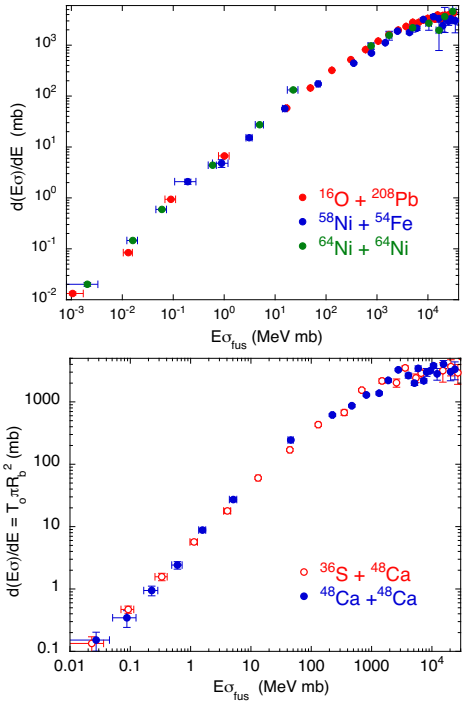

Figure 9. Plot of $d(E\sigma)/dE$ vs $E\sigma$ for ^{16}O + ^{208}Pb [20], ^{58}Ni + ^{54}Fe [15], and ^{64}Ni + ^{64}Ni [2] (top) and for ^{48}Ca,^{36}S + ^{48}Ca [16, 22] (bottom).

energies where the transmission coefficient T_o is one (R_b only weakly depends on E in the measured energy ranges). In the bottom panel of Fig. 9, we see the analogous plot for ^{48}Ca,^{36}S + ^{48}Ca [16, 22] involving very stiff nuclei. The two data sets are very close to each other. The systems considered in Fig. 9 are therefore good starting points to look at the trend of other cases where inelastic excitations and/or nucleon transfer channels have a strong influence on the sub-barrier fusion cross sections.

Using the representation of $d(E\sigma)/dE$ vs $E\sigma$ we now consider the two systems reported in the top panel of Fig. 10. It is well established that in the case of ^{40}Ca + ^{96}Zr [23] nucleon transfer couplings with $Q > 0$ produce large cross section enhancements. This is reflected in the different behaviour with respect to ^{40}Ca + ^{90}Zr [24]. It is evident from Fig. 10 that for the system where transfer couplings are dominant, a smaller derivative $d(E\sigma)/dE$ is observed with respect to the other case (^{40}Ca + ^{90}Zr).

We plot in Fig. 10 (right panel) the behaviour of four other systems where ^{64,60}Ni are involved. We know that the near- and sub-barrier fusion of ^{64,60}Ni + ^{100}Mo are dominated by couplings to the low-lying quadrupole excitation of ^{100}Mo [25, 26], up to the fourth phonon level, while for the two other cases ^{64}Ni + ^{92,96}Zr [27] the important coupled channels are the (weak) quadrupole vibration of ^{92}Zr and the (strong) octupole vibration of ^{96}Zr. Despite their different nature, all these vibrational modes produce fusion excitation functions that, in the $d(E\sigma)/dE$ vs $E\sigma$ representation, have an evident overlap.

The different situations observed in the two panels of Fig. 10 can be explained based on CC model. Indeed, in the lower part of this figure, a simplified view of the predicted barrier distributions [28] for channels with $Q > 0$ (left) and $Q < 0$ (right) is shown. The bottom part is a qualitative picture showing the barrier distribution predicted by the CC model when $Q > 0$ or $Q < 0$ channels are involved. The uncoupled barrier is reduced appreciably by the coupling interaction when $Q > 0$, even if it is reached by only a small fraction of the incident flux. The barrier is less lowered by couplings to channels with $Q < 0$, but it is reached by most of the flux, and the net effect is to produce a simple shift in barrier height, in this case. In other words, the transmission function will be smoother for $Q > 0$ couplings, with respect to $Q < 0$, in particular when the data are plotted in logarithmic scales. The lowest effective barrier will have the largest (smallest) weight for negative (positive) Q values, and $d(E\sigma)/dE$ will be correspondingly larger (smaller).

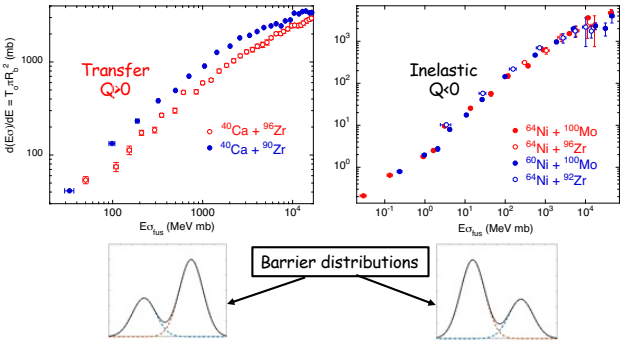

Figure 10. Plot of $d(E\sigma)/dE$ vs $E\sigma$ for ^{40}Ca + ^{90,96}Zr [23, 24] (left) and for ^{64,60}Ni + ^{100}Mo [25, 26] and ^{64}Ni + ^{92,96}Zr [27] (right).

5 Summary

The phenomenon of fusion hindrance has been presented and discussed. In the light systems of astrophysical interest like C+C, O+O and C+O the existence of fusion hindrance is not well established. To clear up their behaviour recent measurements on ^{26,24}Mg, ^{30}Si + ^{12}C have been performed, and the results have been presented here. These three medium-light systems have positive fusion Q-values (similar to the lighter cases) and the hindrance effect shows up at different cross-section levels. In ^{12}C + ^{24}Mg the hindrance threshold is particularly high compared to the available systematics. The underlying reason is not yet clarified and further experimental investigation is necessary.

What we also observe is that far below the barrier, one-dimensional tunnelling calculations reproduce the excitation functions, as if the coupling strengths decrease and tend to vanish. This is not the case with heavier systems where near- and sub-barrier cross section enhancements, being overall larger, are observed even at the lowest measured energies.

A comparative analysis of several systems has been performed using the representation d(Eσ)/dE vs Eσ. This is quite promising because not only it removes the effect of the different Coulomb barriers but it also differentiates the effects of transfer couplings from those of inelastic excitations. The behaviour of various medium-light C + Mg, Si systems indicates that the representation d(Eσ)/dE vs Eσ may be complicated by the existence of cross section

oscillations. Further experiments using γ-particle and ER-particle coincidences are in progress.

Acknowledgements

I am happy to acknowledge the valuable collaboration of Mirco Del Fabbro, Alberto Stefanini and several colleagues of the Laboratori Nazionali di Legnaro and of the Padua Section of INFN. The research leading to the results presented in this talk has received funding from the European Union's Horizon 2020 research and innovation programme, under Grant Agreement No. 654002.

References

[1] C. Jiang, H. Esbensen, K. Rehm, B. Back, R. Janssens, J. Caggiano, P. Collon, J. Greene, A. Heinz, D. Henderson et al., Phys. Rev. Lett. **89**, 052701 (2002)

[2] C. Jiang, K. Rehm, R. Janssens, H. Esbensen, I. Ahmad, B. Back, P. Collon, C. Davids, J. Greene, D. Henderson et al., Phys. Rev. Lett. **93**, 012701 (2004)

[3] G. Montagnoli, A.M. Stefanini, Eur. Phys. J. A **59**, 138 (2023)

[4] C.L. Jiang, B.B. Back, K.E. Rehm, K. Hagino, G. Montagnoli, A.M. Stefanini, Eur. Phys. J. A **57**, 235 (2021)

[5] W.P. Tan, A. Boeltzig, C. Dulal, R.J. DeBoer, B. Frentz, S. Henderson, K.B. Howard, R. Kelmar, J.J. Kolata, J. Long et al., Phys. Rev. Lett. **124**, 192702 (2020)

[6] N.T. Zhang, X.Y. Wang, D. Tudor, B. Bucher, I. Burducea, H. Chen, Z.J. Chen, D. Chesneanu, A.I. Chilug, L.R. Gasques et al., Phys.Lett. B **801**, 135170 (2020)

[7] A.M. Stefanini, G. Montagnoli, M. Del Fabbro, D. Brugnara, G. Colucci, L. Corradi, J. Diklic, E. Fioretto, F. Galtarossa, A. Goasduff et al., Phys. Rev. C **108**, 014602 (2023)

[8] M. Beckerman, Nucl. Phys. A **278**, 333 (1977)

[9] A. Iljinov, M. Mebel, N. Bianchi, E. Desanctis, C. Guaraldo, V. Lucherini, V. Muccifora, E. Polli, A. Reolon, P. Rossi, Nucl. Phys. A **543**, 517 (1992)

[10] C.L. Jiang, B.B. Back, H. Esbensen, R.V.F. Janssens, K.E. Rehm, R.J. Charity, Phys. Rev. Lett. **110**, 072701 (2013)

[11] G. Montagnoli, A.M. Stefanini, C.L. Jiang, K. Hagino, F. Galtarossa, G. Colucci, S. Bottoni, C. Broggini, A. Caciolli, P. Colovic et al., Phys. Rev. C **97**, 024610 (2018)

[12] W. Jordan, J. Maher, J. Peng, Phys.Lett. B **87**, 38 (1979)

[13] C.L. Jiang, K.E. Rehm, B.B. Back, R.V.F. Janssens, Phys. Rev. C **79**, 044601 (2009)

[14] K. Hagino, N. Rowley, A. Kruppa, Comp. Phys. Comm. **123**, 143 (1999)

[15] A.M. Stefanini, G. Montagnoli, L. Corradi, S. Courtin, E. Fioretto, A. Goasduff, F. Haas, P. Mason, R. Silvestri, P.P. Singh et al., Phys. Rev. C **82**, 014614 (2010)

[16] A.M. Stefanini, G. Montagnoli, R. Silvestri, L. Corradi, S. Courtin, E. Fioretto, B. Guiot, F. Haas, D. Lebhertz, P. Mason et al., Phys.Lett. B **679**, 95 (2009)

[17] G. Montagnoli, A.M. Stefanini, C.L. Jiang, K. Hagino, F. Niola, D. Brugnara, P. Colovic, G. Colucci, L. Corradi, R. Depalo et al., J.Phys. G **49**, 095101 (2022)

[18] T. Ichikawa, K. Hagino, A. Iwamoto, Phys. Rev. C **75**, 057603 (2007)

[19] T. Ichikawa, Phys. Rev. C **92**, 064604 (2015)

[20] M. Dasgupta, D.J. Hinde, A. Diaz-Torres, B. Bouriquet, C.I. Low, G.J. Milburn, J.O. Newton, Phys. Rev. Lett. **99**, 192701 (2007)

[21] C.Y. Wong, Phys. Rev. Lett. **31**, 766 (1973)

[22] A.M. Stefanini, G. Montagnoli, R. Silvestri, S. Beghini, L. Corradi, S. Courtin, E. Fioretto, B. Guiot, F. Haas, D. Lebhertz et al., Phys. Rev. C **78**, 044607 (2008)

[23] A.M. Stefanini, G. Montagnoli, H. Esbensen, L. Corradi, S. Courtin, E. Fioretto, A. Goasduff, J. Grebosz, F. Haas, M. Mazzocco et al., Phys.Lett. B **728**, 639 (2014)

[24] H. Timmers, D. Ackermann, S. Beghini, L. Corradi, J. He, G. Montagnoli, F. Scarlassara, A. Stefanini, N. Rowley, Nucl. Phys. A **633**, 421 (1998)

[25] C. Jiang, K. Rehm, H. Esbensen, R. Janssens, B. Back, C. Davids, J. Greene, D. Henderson, C. Lister, R. Pardo et al., Phys. Rev. C **71**, 044613 (2005)

[26] A.M. Stefanini, G. Montagnoli, F. Scarlassara, C.L. Jiang, H. Esbensen, E. Fioretto, L. Corradi, B.B. Back, C.M. Deibel, B. Di Giovine et al., Eur. Phys. J. A **49**, 63 (2013)

[27] A.M. Stefanini, L. Corradi, D. Ackermann, A. Facco, F. Gramegna, H. Moreno, L. Mueller, D.R. Napoli, G.F. Prete, P. Spolaore et al., Nucl. Phys. A **548**, 453 (1992)

[28] C. Dasso, S. Landowne, A. Winther, Nuclear Physics A **407**, 221 (1983)